# SLAFEX 2024: Current vs voltage characteristic in an $Al_{0.1}In_{0.9}As/InAs_{0.09}N_{0.01}/Al_{0.1}In_{0.9}As$ double-barrier heterostructure

H. Paredes and C. L. Beltrán Ríos

*Escuela de Física, Universidad Industrial de Santander SAN-680002,*
*Bucaramanga, Colombia, ORCID 0000-0001-6515-4746.*
*e-mail hparedes@uis.edu.co; cbeltran@uis.edu.co*

Received 28 October 2024; accepted 11 November 2025

This article reports the study of the characteristic behavior of current in function of applied voltage for a double-barrier heterostructure (DBH) of InAsAl/InAsN/InAsAl, considering low Nitrogen concentrations ($< 1\%$) for different temperature values and with a magnetic field applied parallel and/or perpendicular to the double barrier system. This work used the theory of non-equilibrium Green's function (NEGF). The current-voltage curves show new resonant states due to the incorporation of Nitrogen in the quantum well and the intensity of these peaks diminishes with the increased temperature. In addition, our results show that the effect of the applied magnetic field perpendicular to the current is stronger compared with the applied magnetic field parallel to the current, yielding a behavior similar to the experimental data by Di Paola [Sci. Rep. 2016; 6, 32039].

*Keywords:* Current; voltages; tunneling; impurity; double barrier.

DOI: https://doi.org/10.31349/RevMexFis.72.030504

## 1. Introduction

Currently, the fabrication of semiconductor heterostructures by materials from groups III and V of the periodic table with low concentrations of Nitrogen N has been considered of great interest. These systems have shown new resonant states, creating new possibilities to develop optoelectronic devices for use in detection or emission at mid-infrared wavelengths. These properties have been reported in diverse experimental [1-8] and theoretical [9,10] articles. Shih *et al.*, [1] conducted a study on samples of InAsN block layers with different N concentrations, with their results showing that the absorption energy of InAsN is higher than that of InAs and the bandgap energy of InAsN decreases as the N concentration increases, besides finding an increase in the effective mass of electrons in these InAsN alloys. Magnetoresistance measurements and Hall effect studies on $InAs_{1-x}N_x$ layers, grown on a GaAs substrate, show that electron mobility is in the order of $6 \times 10^3$ $cm^2V^{-1}s^{-1}$ at 300 K. Cyclotron resonance studies showed a systematic increase in the cyclotron mass of electrons, with increased N concentration [2,3]. Hang *et al.*, [4] investigated the Shubnikov-de Haas oscillations of a two-dimensional electron gas in quantum wells (QWs) of $InAs_{1-x}N_x$/InGaAs, with low N content and an applied magnetic field, finding that the effective mass of electrons increases and the carrier mobility is markedly decreased when incorporating a small amount of N; this is mainly due to the modification of the band structure induced by nitrogen. Photoreflectance spectroscopy has been used to study the energy gap and spin-orbit coupling in $InAs_{1-x}N_x$ alloys with $0 < x < 0.88$ %. Kudrawiec *et al.*, [5] indicate in their result that incorporating approximately 1% N in InAs reduces the energy gap around 60 meV. In photoluminescence (PL) spectrum studies in InAsN alloys, which contain up to 1% N, localized states were observed within the conduction band. In addition, the intensity of the PL emission peaks of the samples containing N are higher than in the InAs samples [6]. From the PL spectrum data, dependence on the bandgap energy in function of N concentration is observed, showing its decrease as N content increases [7]. Kuroda *et al.*, [8] conducted a study on InAsN films in block and single quantum well (SQW) of InAsN/GaAs with high N concentrations. In their experimental results, they found that as N concentration increased: i) the optical absorption spectrum is blue-shifted due to the Burstein-Moss (BM) effect. This effect is dominant near the edge of the band in InAsN films; ii) the PL spectrum shows a red-shift due to the bandgap narrowing and the BM effect is negligible in the InAsN/GaAs SQWs. Benaissa *et al.*, [9] using ab-initio methods, calculated the lattice constant as a function of the N concentration ($0 < x < 0.14$); a deviation from Vegard's law is observed in their results for the variation of the InAsN lattice constant. The lattice parameter calculated in the order of 5.97 Å agrees with the experimental value of 6.0 Å at a concentration of $x = 0$. In addition, they calculated the energy gap, finding its decrease with increased aluminum concentration. Gueddim and Bouarissa [10] studied the electronic band structure of ternary dilute $InAs_{1-x}N_x$ alloys, using the pseudopotential method, they reported the dispersion relation for the system, showing that it is a direct gap semiconductor material. With respect to the electronic and optical properties, their results showed that the effective masses of electrons and heavy holes, dielectric constants at high frequency and static vary non-linearly with increasing N concentration.

In the last decade, Zener tunneling has been observed due to the transport of electrons from the valence band to the con-

duction band and new properties appearing in III-V semiconductors when N atoms are incorporated, propitiating possible new applications in optoelectronic devices [11, 12]. Di Paola *et al*., [11] conducted the study on InAsAl/InAsN/InAsAl double-barrier resonant tunneling diodes (RTDs); in their report of the characteristic current vs. voltage curves, a peak is observed at a voltage $V \approx 0.06$ V, originated by the incorporation of N in the QW; new states, created by the presence of Nitrogen, these states permit the resonant tunneling of electrons that cross the potential barrier in the RTD giving rise to a negative differential resistance. Transport studies in organic Zener diodes [12] show that the tunneling current depends on the thickness of the intrinsic interlayer and the doping concentration of the electron and hole transport layers. In the current vs. voltage curves it was observed that for positive voltage values, the current behaves similar to a diode. Instead, a significant effect on the current appears as the reverse breakdown voltage changes $-3$ to $-15$ V with increasing thickness of the devices intrinsic interlayer.

A. Tibaldi, *et al*. [13], performed numerical simulations on a resonant tunnel diode (RTD) consisting of a 5 nm $In_{0.53}Ga_{0.47}As$ quantum well sandwiched between 1.5 nm thick AlAs barriers. Using non-equilibrium Green's functions, they calculated the steady-state current as a function of the voltage with and without scattering mechanisms for different temperatures. The I-V curves show a reduction in the peak current intensity with increasing temperature; this can be almost entirely attributed to carrier phonon scattering and resonant states broadening. Żak *et al*. [14], studied the resistivity for tunnel junctions in a (In,Ga)N quantum well (QW) sandwiched between $In_{0.02}Ga_{0.98}N$ barriers, the quantum well is doped with Silicon and Magnesium;this work show a diminishing in the voltage with increasing the doping for both Silicon and Magnesium, increasing the tunneling current across the junction. Masanori Nagase [15] performed a theoretical study of the peak-to-valley current relationship (PVCR) in GaN/AlN resonant tunnel diodes (RTDs); this results for the I-V characteristic curves show two peaks associated with the three-dimensional and two-dimensional (3D-2D) and 2D-2D resonant tunnel currents; 2D-2D resonant tunneling peaks are sharper than the 3D-2D resonant tunneling peaks, author considered that this behavior is associated to the changed phase coherence length of electrons, This, in turn, it was associated to the probability of electronic phase relaxation or electronic scattering in the quantum well.

In this article we report a theoretical study of resonant interband tunneling, using the general approach of non-equilibrium Green's function of current as a function of voltage, temperature, and parallel and perpendicular magnetic field in an InAsAl/InAsN/InAsAl DBH. Our results are similar to previous works, especially with the experimental work reported in Ref. [11].

## 2. Theory

To describe the characteristic current vs voltage for a DBH, the study followed the theoretical model proposed by R. Golizadeh-Mojarad and S. Datta [16]. Current through the DBH is given by:

$$I = \frac{e}{\hbar}\int_{-\infty}^{+\infty} T(E)(f_L(E) - f_R(E))dE\,, \tag{1}$$

where $f_{(L,R)}(E)$ is the Fermi function of the contacts to the left (L) and right (R) of the structure and $T(E)$ is the effective transmission function that in the NEGF method is give by

$$T(E) = \text{Trace}[\Gamma_1 G \Gamma_2 G^{+}], \tag{2}$$

where $G$ is the Green function matrix for the system give by

$$G(E) = [EI - H - \Sigma_1 - \Sigma_2]^{-1}, \tag{3}$$

and

$$\Gamma_{1,2} = \imath(\Sigma_{1,2} - \Sigma_{1,2}^{+}), \tag{4}$$

where $I$ is the identity matrix, $H$ is Hamiltonian matrix of the isolated device region and $\Sigma_{1,2}$ are the matrix that represent the lead effect. The Hamiltonian matrix of the system is described through Eq. (5) [17].

$$H(i,j) = \begin{cases} zt + U(i,j) + \hbar\omega_i & ; i = j \\ -\tilde{t}_{i,j} & ; i \neq j, \text{ nearest neighbors} \\ 0 & ; \text{ other cases} \end{cases}, \tag{5}$$

where $t = \hbar^2/2ma^2$, $m$ is the effective mass of the electron, $a$ is the lattice constant, $z$ represents the number of nearest neighbors ($z = 2$ for the 1D model), and $U$ represents the potential profile of the DBH (Fig. 1). The effect of the applied magnetic field perpendicular to the current is taken into account through Eq. (6) [18].

$$\tilde{t}_{i,j} = t\,\exp\left[\imath\, e\,\mathbf{A}\left(\frac{\mathbf{r}_i + \mathbf{r}_j}{2}\right)\cdot(\mathbf{r}_i - \mathbf{r}_j)\,a\right], \tag{6}$$

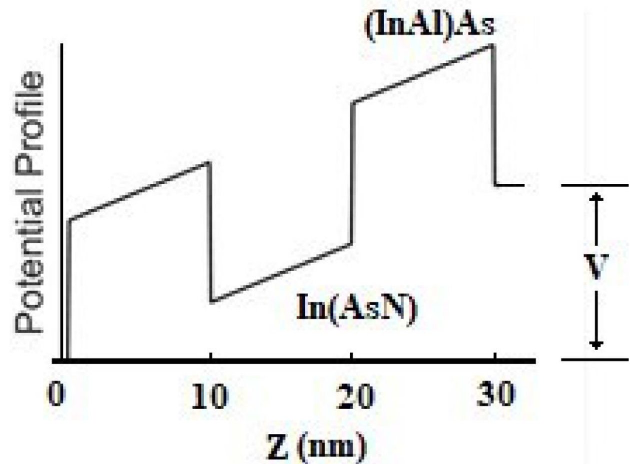


FIGURE 1. Conduction band profile for a DBH with a V bias applied, 10-nm wide for the InAsN QW and 10-nm wide for the InAsAl barriers. Barrier heights between InAs/(InAl)As of 0.12 eV and In(AsN)/(InAl)As of 0.16 eV, respectively.

with **A** being the described potential vector , in coordinates (x, y, z), $\mathbf{A} = Bz\,\mathbf{e}_x$ ($\mathbf{B} = B\,\mathbf{e}_y$). $\mathbf{r}_i$ and $\mathbf{r}_j$are the position vectors for sites i and j of the nearest neighbor atoms, at all lattice positions. The applied magnetic field parallel $\mathbf{B} = B\mathbf{e}_z$ to the direction of the current is taken into account in the diagonal term at the Eq. (5) as $\varepsilon_i = (n + [1/2])\,\hbar\omega_i$ , [19] where $n$ corresponds to Landau Level and $\omega_i$ is the cyclotron frequency given by

$$\omega_i = \frac{e\,B}{m_i\,c}, \tag{7}$$

and $m_i$ is the electronic effective mass on the *x*-*y* plane, $e$ is the electron charge, $B$ is the applied magnetic field, and $c$ is the speed of light.

## 3. Results and discussion

To study resonant interband tunneling in an InAsAl/InAs N/InAsAl DBH connected to two identical InAs contacts to the left (L) and right (R) of the system, we have considered an electron concentration of $n = 2 \times 10^{17}$ cm$^{-3}$ in the emitter, corresponding to a Fermi energy of 49.8 meV. It is deemed that the height of the potential between contact L of InAs to the (InAl)As barrier as 0.12 eV, with 10% Al content and 10-nm barrier width; the height of the potential between the In(AsN) QW to the (InAl)As barrier is 0.16 eV, with 1% N content and 10-nm QW width, as seen in Fig. 1.

The resonant tunneling process under study consisted of light holes (we did not consider heavy-hole tunneling) tunneling from the emitter to the collector through resonant states created in the quantum well by the N atoms; the parameters used in this work are effective mass of the light hole in the InAs, $m_{lh} = 0.027\,m_0$ [19], the effective mass and constant lattice of the contact L (R) of InAs are $m_{L(R)} = 0.025\,m_0$ [11] and $a_{L(R)} = 6.058$Å [20], the effective mass and the lattice constant at the (InAl)As barriers, $m_b = 0.039\,m_0$ [11] and $a_b = 5,97$ Å [21], the effective mass and lattice constant

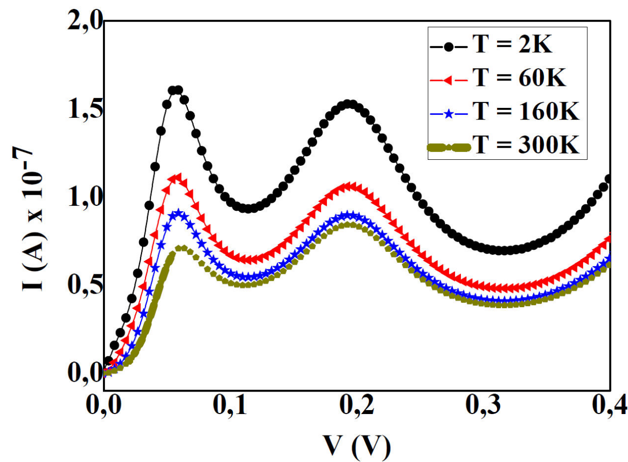


FIGURE 2. $I$ vs. $V$ characteristic for a double-barrier system as function of temperature of 2, 60, 160, and 300 K without applied magnetic field.

in the In(AsN) well $m_w = 0.026\,m_0$ [11] and $a_w = 5.96$ Å [9], and $m_0$ is the mass of the free electron, respectively.

Current $I$ as a function of applied voltage $V$ for an InAsAl/InAsN/InAsAl DBH with different temperature values and zero magnetic field is shown in Fig. 2, an increase and diminish in current is observe when the voltage applied to the system is increase. In this figure it can be observe that the current reaches a first peak at 0.059 V and then it drops (a region of negative differential resistance) with increased voltage; as voltage continues to increase, a second peak of magnitude slightly smaller than the first is noted at 0.19 V. The first peak is associated to the incorporation of the Nitrogen in small concentrations ( 1%) into the InAs, as reported by Di Paola *et al.*, [11] causing the decrease in the bandgap energy creating resonant levels, which allows the tunneling of electrons through the states located in the energy gap of the InAsN layer [11, 22]. The second peak is due to the resonant states in the InAsN quantum well as applied voltage increases. Further, it is observed in Fig. 2 that current peaks diminish as temperature increases. As reported by Di Paola *et al.*, [11] the contacts between which the double-barrier structure is found are n-type and p-type, on the left and right of the system, respectively, allowing charge carriers to tunnel through states in these zones favoring conduction. These are also affected by effects of temperature and applied voltage. To model this, it may be considered that the chemical potential of the contacts in our double-barrier system are misaligned, with the one on the right being higher than the one on the left, as applied voltage increases. The effect of temperature causes a redistribution of the charge, making the states associated with the contacts to contribute fewer carriers through recombination than can occur with the n-type and p-type layers of the system. In this study we are obtained qualitative results similar to those reported by the experimental work by Di Paola *et al.*, [11].

Figure 3 presents the characteristic $I$ vs. $V$ curves for different magnetic fields perpendicular (a) and parallel (b) to the direction of the current for temperature $T = 2.0$ K. For the perpendicular field, a decrease in the current intensity is observed with the increased applied field; the first peak tending to disappear at a value of 3.0 T. With the magnetic field parallel to the current, the decrease of the peaks is negligible compared with the intensity of the peaks with perpendicular field; furthermore, the peak in the case of the parallel field undergoes a shift at higher energy values, with the applied bias. This could be associated with the additional confinement introduced by the magnetic field in the charge carriers.

Figure 4 shows the $I$ vs. $V$ curves for different temperatures with a 1 T magnetic field parallel (left) and perpendicular (right) to the current. Note the presence of two peaks, one due to the presence of the low N concentration that creates levels in the gap and permits electron tunneling and the other peak due to resonant states in the QW, as described in Fig. 2. As temperature increases, the intensity of both peaks diminishes. It is observed that the intensity of the second peak is greater than that of the first; this is best observed in the case

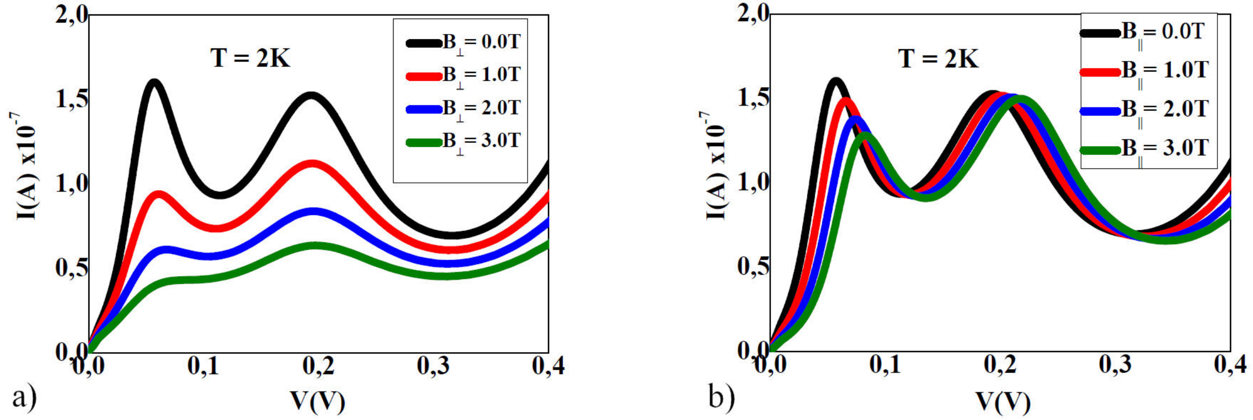


FIGURE 3. $I$ vs. $V$ for a double-barrier system in the presence of a magnetic field perpendicular a) and parallel b) to the direction of the current for different values of $B$ ($B = 0$, 1.0, 2.0, 3.0 T) at temperature $T = 2$ K.

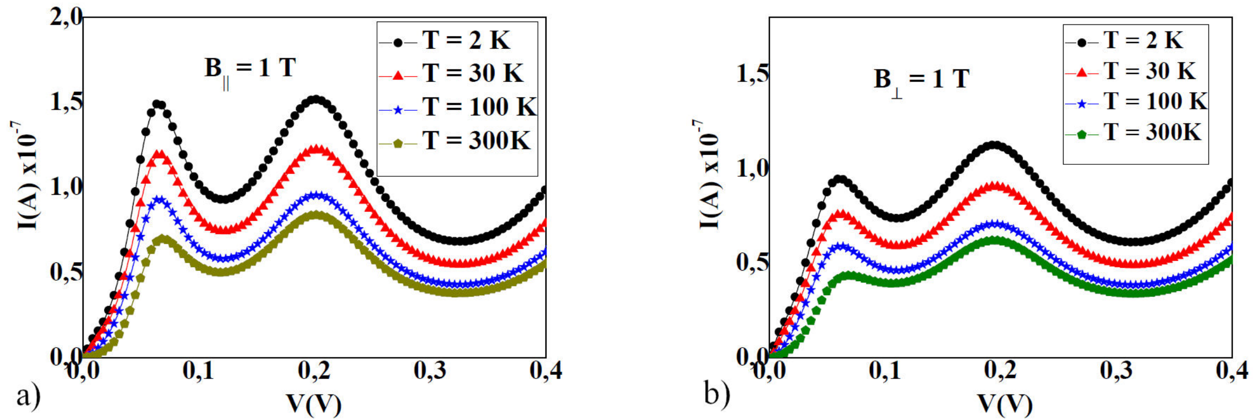


FIGURE 4. $I$ vs. $V$ for a double-barrier system in presence of a parallel ($B_{\|}$) and perpendicular ($B_{\perp}$) magnetic field of $B = 1$ T, for different temperatures $T = 2$, 30, 100, and 300 K.

of the perpendicular field. The first peak is associated with more localized wave functions and the second peak with wave functions more extended in the direction perpendicular to the growth of the structure. This could cause greater overlap of the wave functions of the carriers. Also, it can be noted that the second peak is more intense than the first peak, given that the magnetic field introduces additional confinement of the charge carriers and this effect is not seen in Fig. 2, which is without applied magnetic field.

In the above figures, the appearance of the first peak coincides with the level of energy obtained by solving Schrodinger's equation of the steady state for a quantum well structure of InAs/$InAs_{0.9}Al_{0.1}$ and well structure of InAs(N)/$InAs_{0.9}Al_{0.1}$, finding a single level without applied magnetic field. The value obtained of the energy of the level, taking into account the differences of effective masses among the carriers in the well and the barrier, are shown in Table I.

As seen in Table I, the second column corresponds to the solution of the Schrodinger's equation by means of the odeint method in scipy library [23] from python [24], the value obtained for the well level is closer to the value at which the first peak is observed in the $I$ vs. $V$ curves, both for this work as for that reported by Di Paola *et al.*, [11]; hence, it is clear that the first peak observed in the $I$ vs. $V$ curves is associated with the Nitrogen impurity in the InAs well. The third column corresponds to the values obtained by applying the boundary conditions on the quantum well structure, considering the differences in electron masses between the well and the potential barrier [25]; the fourth column in the table corresponds to the solution of Schrodinger's equation by using the finite differences method [26].

TABLE I. Quantum well level energy values. The $V_b$ values correspond to the barrier height for electrons in the quantum well

| Well/barrier structure | SciPy ODEINT | Transcendental equation | Finite differences |
|---|---|---|---|
| InAs/$InAs_{0.9}Al_{0.1}$ ($V_b = 0.12$ eV) | 54.1 (meV) | 41.9 (meV) | 42.2 (meV) |
| InAs(N)/$InAs_{0.9}Al_{0.1}$ ($V_b = 0.16$ eV) | 59.6 (meV) | 47.3 (meV) | 47.6 (meV) |

## 4. Conclusions

This theoretical work studied current vs. voltage and reproduced well the position of the first peak associated with the incorporation of Nitrogen in small concentrations (1%) into InAs and showed a decrease in current as temperature decreased, compared with the experimental report [11]. Moreover, it is noted in curves $I$ vs. $V$ a weak effect of the applied magnetic field parallel to the current, compared with the applied magnetic field perpendicular to the current. With the incorporation of nitrogen in these devices, new resonant states and a region of negative differential resistance that is weakly affected by temperature have been observed, these states would make the possibility for the development of optoelectronic devices.

## Acknowledgements

This work was funded by Universidad Industrial de Santander (UIS) through the Vice-rectory of Research, via Research Project: No. 2414.

1. D.K. Shih, H.H. Lin, L.W. Sung, T.Y. Chu, and T.R. Yang, Band gap reduction in InAsN alloys, *Jpn. J. Appl. Phys.* **42** (2003) 375, https://doi.org/10.1143/JJAP.42.375
2. A. Patanè *et al*., Effect of low nitrogen concentrations on the electronic properties of $InAs_{1-x}N_x$, *Phys. Rev. B* **80** (2009) 115207, https://doi.org/10.1103/PhysRevB.80.115207
3. O. Drachenko *et al*., Cyclotron resonance mass and Fermi energy pinning in the In(AsN) alloy, *Appl. Phys. Lett.* **98** (2011) 162109, https://doi.org/10.1063/1.3583378
4. D.R. Hang *et al*., Large effective mass enhancement of the $InAs_{1-x}N_x$ alloys in the dilute limit probed by Shubnikov-de Haas oscillations, *Physica E* **22** (2004) 308, https://doi.org/10.1016/j.physe.2003.12.008
5. R. Kudrawiec, J. Misiewicz, Q. Zhuang, A. M. R. Godenir, and A. Krier, Photoreflectance study of the energy gap and spin-orbit splitting in InNAs alloys, *Appl. Phys. Lett.* **94** (2009) 151902, https://doi.org/10.1063/1.3117239
6. M. de la Mare, Q. Zhuang, A. Krier, A. Patanè, and S. Dhar, Growth and characterization of InAsN/GaAs dilute nitride semiconductor alloys for the midinfrared spectral range, *Appl. Phys. Lett.* **95** (2009) 031110, https://doi.org/10.1063/1.3187534
7. J. Ibáñez *et al*., Structural and optical properties of dilute InAsN grown by molecular beam epitaxy, *J. Appl. Phys.* **108** (2010) 103504, https://doi.org/10.1063/1.3509149
8. M. Kuroda, A. Nishikawa, R. Katayama, and K. Onabe, Growth and characterization of InAsN alloy films and quantum wells, *J. Crystal Growth* **278** (2005) 254, https://doi.org/10.1016/j.jcrysgro.2005.01.075
9. H. Benaissa, A. Zaoui, and M. Ferhat, First principles calculations for dilute $InAs_{1-x}N_x$ alloys, *J. Appl. Phys.* **102** (2007) 113712, https://doi.org/10.1063/1.2821144
10. A. Gueddim and N. Bouarissa, Electronic structure and optical properties of dilute $InAs_{1-x}N_x$: pseudopotential calculations, *Phys. Scr.* **80** (2009) 015701, https://doi.org/10.1088/0031-8949/80/01/015701
11. D. M. Di Paola *et al*., Resonant Zener tunnelling via zero-dimensional states in a narrow gap diode, *Sci. Rep.* **6** (2016) 32039, https://doi.org/10.1038/srep32039
12. H. Kleemann *et al*., Organic Zener diodes: tunneling across the gap in organic semiconductor materials, *Nano Lett.* **10** (2010) 4929, https://doi.org/10.1021/nl102916n
13. A. Tibaldi, M. Goano, and F. Bertazzi, Small-signal modeling of dissipative carrier transport in nanodevices with nonequilibrium Green's functions, *Phys. Rev. Applied* **19** (2023) 064020, https://doi.org/10.1103/PhysRevApplied.19.064020
14. ] M. Żak *et al*., Tunnel junctions with a doped (In,Ga)N quantum well for vertical integration of III-nitride optoelectronic devices,*Phys. Rev. Applied* **15** (2021) 024046, https://doi.org/10.1103/PhysRevApplied.15.024046
15. M. Nagase, Theoretical analysis of current-voltage characteristics of GaN/AlN resonant tunneling diodes including electron phase relaxation in quantum well, *Jpn. J. Appl. Phys.* **64** (2025) 061002, https://doi.org/10.35848/1347-4065/addd79
16. R. Golizadeh-Mojarad and S. Datta, Nonequilibrium Green's function based models for dephasing in quantum transport, *Phys. Rev. B* **75** (2007) 081301, https://doi.org/10.1103/PhysRevB.75.081301
17. S. Datta, in Quantum Transport: Atom to Transistor, *edited by Cambridge University Press* (2005) p. 145.
18. H. Paredes Gutiérrez, N. Porras-Montenegro and A. Latgé, Magnetic field and hopping effects on the current-voltage characteristics in a GaAs/AlxGa1-xAs double-barrier heterostructure, *Phys. Rev. B* **68** (2003) 045311, https://doi.org/10.1103/PhysRevB.68.045311
19. M. A. Davidovich, Effects of carrier mass differences on the I-V characteristics of resonant interband tunneling structures in the presence of parallel magnetic field, *J. Appl. Phys.* **78** (1995) 5467, https://doi.org/10.1063/1.359662
20. I. Vurgaftman, J. R. Meyer and L. R. Ram-Mohan, Band parameters for III-V compound semiconductors and their alloys, *J. Appl. Phys.* **89** (2001) 5815, https://doi.org/10.1063/1.1368156
21. M. Ameri *et al*., Ab initio calculations study of structural and electronic properties of ternary alloy $Al_xIn_{1-x}As$, *Materials Sciences and Applications*, **3** (2012) 674, https://doi.org/10.4236/msa.2012.310099
22. E. P. O'Reilly, A Lindsay, P. J. Klar, A. Polimeni and M. Capizzi, Trends in the electronic structure of dilute nitride alloys, *Semicond. Sci. Technol.* **24** (2009) 033001, https://doi.org/10.1088/0268-1242/24/3/033001

23. P. Virtanen *et al*., SciPy 1.0: Fundamental Algorithms for Scientific Computing in Python, *Nature Methods* **17**, 261-272 (2020).https://doi.org/10.1038/s41592-019-0686-2

24. G. Van Rossum and F. L. Drake Jr, *Python reference manual* (Centrum voor Wiskunde en Informatica Amsterdam, 1995). https://dl.acm.org/doi/book/10.5555/1593511

25. G. T. Einevoll and L. J. Sham, Boundary conditions for envelope functions at interfaces between dissimilar materials, *Phys. Rev. B*, **49** (1994) 10533, https://doi.org/10.1103/PhysRevB.49.10533

26. P. A. Belov and E. S. Khramtsov, The binding energy of excitons in narrow quantum wells, *IOP Conf. Ser. Journal of Physics. Conf. Series* **816** (2017) 012018, 10.1088/1742-6596/816/1/012018.